New Magnetic Co_3O_4/Fe_3O_4 Nanoparticles Doped Polyaniline Nanocomposite for The Effective and Rapid Removal of Nitrate Ions from Underground Water Samples

Mohammad Ali Gabris[1], **ZeinabAsadi[2]**,, Binta Hadi[4], Mehdi Esmaeili Bidhendi[1, 2*], Rashmin Khanam[6*] ,Syed Shahabuddin[5]* and Saidur Rahman[5,7]

[1]*Department of Chemistry, Faculty of Science, University of Tehran, Iran*

[2]*Department of Environment, Kish International Campus, University of Tehran, Kish Island, Iran*

[3]*Graduate Faculty of Environment, University of Tehran, Tehran, Iran*

[4]*Department of Chemistry, Aljouf University Sakaka, 72388, Aljouf Region, KSA*

[5]*Research Centre for Nano-Materials and Energy Technology (RCNMET), School of Science and Technology, Sunway University, 47500 Selangor Darul Ehsan, Malaysia*

[6] *Centre for Interdisciplinary Research in Basic Sciences, Jamia Millia Islamia, New Delhi 110025, India.*

[7]Department of Engineering, Lancaster University, Lancaster, LA1 4YW, United Kingdom

*Corresponding Authors: Dr. Syed Shahabuddin(syedshahab.hyd@gmail.com; syeds@sunway.edu.my), Dr. Mehdi Esmaeili (esmaeilib@ut.ac.ir) and Dr. Rashmin Khanam (Rashmin.jmi@gmail.com)

Abstract

In the present study, a new nanocomposite of iron/cobalt oxides and magnetic nanoparticle doped with polyaniline (**PANI-Co_3O_4@MNPs**) was synthesized and subsequently, evaluated for its potential in decontaminating nitrate ions from underground water. Various parameters such as pH, mass dosage, adsorption time, initial concentration and temperature important in obtaining optimum conditions required to attain maximum performance for the reported nanocomposite in nitrate removal were experimentally investigated. The important surface and chemical properties of **PANI-Co_3O_4@MNPs** including surface morphology and roughness, composition and chemical structure were evaluated using various spectroscopic techniques such as Field Emission Scanning Electron Microscope (FE-SEM), Energy-Dispersive X-ray spectroscopy (EDX) and Fourier Transform Infrared (FTIR). Finally, the removal of nitrate was assessed using kinetic, adsorption isotherm and thermodynamic studies to investigate the underlying mechanism of the removal process into **PANI-Co_3O_4@MNPs** sorbent**.** The kinetic studies and the adsorption isotherms have been well explained using pseudo first and the Freundlich models respectively whereas the thermodynamic parameters have been described in terms of enthalpy, entropy and Gibbs free energy which showed a negative value signifying that the adsorption process was exothermic and spontaneous in nature.

Keywords: Nanocomposite; NitrateRemoval; Iron Oxide; CobaltOxide; Polyaniline

1. Introduction

The abrupt increase in population and industries have substantially increased the environmental pollution, particularly nitrates which contaminates the underground water resources leading to malicious damage [1],[2].The main sources of nitrate embraces a wide variety of waste water septic systems, different kinds of fertilizers, industrial sewage and animal manures [3],[4]. Nitrates certainly causes harm to the ecosystem and the various living organisms [2] leading to many contagious diseases including infant methemoglobinemia (blue baby syndrome) [1],[5],[6],[7], cancer [5],[6],[7],[8],[1], eutrophication [7], diabetes [8], etc,. The permissible limits for nitrate-nitrogen (NO_3-N) in drinking water has been set by World Health Organization (WHO, 2008) and USEPA (EPA) as 50 mg/l and 10 mg/l, respectively [3]. Recently, the research related to the removal of nitrate from aquatic environment has been increased significantly. Several physical, chemical and biological processes have been developed; however, some of the reported conventional and physical methods such as filtration are considered inappropriate for nitrate removal. Techniques like

adsorption [8], [9], [10], [11], ion exchange [12], [13], [8], catalytic reduction using monometallic [14] or bimetallic particles [15], photocatalytic reduction, reverse osmosis [8], [10,] [16], electrodialysis [10], electrochemical methods [8], [17], [18], biological and [8],[19],[20],[21] chemical denitrification [8].[22],[23] have been effectively used for removal of nitrate. Almost all aforementioned techniques except adsorption, suffers various technical drawbacks such as secondary pollution from bacteria or chemicals, technical complexity, low efficiency, requirement of post-treatment, high dependency on nitrate amount and high energy demand on large-scale for water treatment plants that restricts their applicability [8],[24].

On the other hand, adsorption displays high efficiency and low cost which makes it the most suitable technique for nitrate removal [3],[25],[26],[27],[28]. Nanomaterials due to their very small sizes possess some of the unique properties like large surface area, high reactivity, easy synthesis, good electrical conductivity and high catalytic activity. Moreover, adsorption process is also useful in separation, retrieval and recycling of the nanomaterials [8]. Different nanocomposites such as polymers, magnetic polymers, graphene based materials and activated carbons act as effective nitrate removal [8],[23],[29],[30]. Conducting polymers such as polyaniline, polythiophene, polyacetylene and polyethylene have been synthesized as organic-inorganic hybrid nanocomposite materials and because of their inimitable potentials and unique electrical, optoelectronic and chemical properties attributed to the presence of extended π-conjugated electron system along the backbone of the conjugated materials they are used in many scientific researches related to sensors, batteries, electronics, electromagnetism, electro-luminescence, thermoelectricity and electro-mechanics [31],[32],[33]. Among the several conducting polymers, polyaniline (PANI) has been known to be as a highly effective adsorbent because of its important properties like high surface area, easy preparation, positive surface charge, distinctive electrochemical performance, environmental stability and reusability. However, the use of PANI in many environmental applications is limited owing to its poor mechanical properties and solubility [32]. Thus, by blending PANI into a flexible host matrix with enhanced chemical stability towards dopants, high electrical conductivity and thermal stability can be achieved [34],[35]. It is noteworthy that the mechanical property of PANI can considerably be improved by integrating it with oxides of Iron and Cobalt. Cobalt oxide nanoparticles (Co_3O_4) is a magnetic π-type semiconductor belonging to the important class of inorganic metal oxides of normal spinel structure with cubic close packing array of the oxide ions. Above all, this nanomaterial also possess the magnetic character offering its easy recovery by an external magnet along with the other crucial features offacile synthesis, diverse morphology, perfect catalytic ability[36],eclectic availability and cost effectiveness which enhance its utilization in fuel cells, photocatalysis, lithium batteries, gas sensors, artificial photosynthesis and etc.[37].

In this study, a novel nanocomposite consisting of iron/cobalt oxide nanoparticles doped with polyaniline (**PANI-Co_3O_4@MNPs**) has been synthesized to assess its potency in removal of nitrate from real underground water samples. The synthesized material was comprehensively characterized and various important parameters were evaluated experimentally. The various well-known kinetic and adsorption isotherm models were applied to evaluate and optimized the adsorption experimental data. The thermodynamic parameters were also estimated for the removal process. The results suggested that the new nanocomposite act as potent absorbent for effective removal of nitrate ions from the contaminated underground water samples.

2. Experiments

2.1 Chemicals and Reagents

Ammonium persulfate (APS), cobalt acetate tetrahydrate, methanol, ammonia solution, hydrochloric acid and aniline were bought from R & M chemicals (London, UK). Ferrous chloride tetrahydrate, ferric chloride hexahydrate and aniline were purchased from Merck (Darmstadt; Germany). Aniline was distilled and kept in a dark place before use. Underground water was collected from south of Iran.

2.2 Spectroscopic Analysis

IR spectra for all synthetic compounds were taken on Perkin Elmer RX1 FTIR-ATR spectrometer (MA, USA) and wave numbers were calculated in cm^{-1}.The surface morphology of **PANI-Co_3O_4@MNPs** nanocomposite was studied using TESCAN MIRA3 field emission scanning electron microscopy, FESEM (Prague, Czech Republic). The concentration of Nitrate ions in aqueous solution was measured using Perkin Elmer Lamda 5 double beam ultraviolet spectrometer (MA, USA) at λ_{max} 350 – 600 nm taking tungsten lamp as the source of light (Fisher Scientific, USA).

2.3 Synthesis of PANI-Co_3O_4@MNPs nanocomposite

Cobalt oxide (Co_3O_4) nanoparticles were synthesized according to the previously reported protocol [36][32]. Polyaniline doped Co_3O_4 nanocomposite was prepared as follows; 10 g of aniline was taken and dissolved in 50 mL (1M) HCl solution and was kept for stirring for about 30 minutes in an Erlenmeyer flask. 1g of Co_3O_4 nanoparticles were dispersed in distilled water and sonicated for 30 minutes in different vial. The cobalt solution was then added dropwise to the aniline solution followed by vigorous stirring for 1 h. The crude product (PANI-Co_3O_4) was then filtered and washed carefully to carry out further experiments. Next step was to magnetize the produced nanocomposite, for which, 5 g of PANI-Co_3O_4, 2 g of $FeCl_2.4H_2O$ and 1 g of $FeCl_3.6H_2O$ were mixed together in 50 mL of distilled water and left for sonication for 30 minutes to obtain a homogenous solution. Thereafter, the

solution was heated to 40-50°C and 3 mL of ammonia solution (25%) was added to the mixture and stirred for 5 hours. The dark colored product (PANI-Co_3O_4@MNPs) so obtained was washed thoroughly with excess of water and dried in oven for 24 hours at 80°C.

2.4 Removal Procedure

The initial concentration of nitrate in the tested underground water was found to be 48.5 ppm. The removal of nitrate from the given samples was done through addition of 20 mg of sorbent (**PANI-Co_3O_4@MNPs**) to 20 mL sample for 30 minutes with constant shaking at room temperature. Various experimental parameters such as pH of the sample (2-10), dosage of sorbent (5-150 mg), contact time (5-150 min), initial concentration of nitrate (1-25 mg/L) and adsorption temperature (20°C, 25°C, and 35°C) were measured and set to optimal. After adsorption, the residual amount of nitrate in solution was measured using UV-Vis spectrophotometer at 220 nm. Finally, equations (1) and (2) were used to estimate the removal percentage (R%) and the equilibrium adsorption capacity (Qe), respectively[21].

$$R\,\% = \left(\frac{C_0 - C_e}{C_0}\right) \times 100 \qquad (1)$$

$$Q_e = \frac{V}{m}(C_0 - C_e) \qquad (2)$$

where Q_e, C_0, C_e, V and m represents the adsorption capacity (mg/g), initial and residual concentrations of nitrate (mg/L), volume of solution (mL) and adsorbent mass (g) respectively.

3 Results and discussion

3.1 Spectroscopic Analysis

3.1.1 FESEM microscopy

To evaluate the size and morphology of cobalt oxide nanocubes, PANI and PANI-Co_3O_4 nanocomposite, the field emission scanning electron microscopy (FE-SEM) was used before and after activation. The PANI so synthesized was compared with that of the reported in literature. The spectral images showed visible modifications and changes in the surface morphology of plain PANI when doped with oxides. These changes affect the surface properties of the material as whole and lead to an increase in the adsorption capacity of the nanocomposite. Fig. 1 represented the morphology of cobalt oxide nanoparticles at various magnifications. These images clearly indicated the formation of

cube-shaped cobalt oxide nanoparticles with a uniform shape and size. The implanted nanoparticles displayed aggregation [38], exhibited spherical shape and unevenly distributed all over the relatively smooth surface of PANI polymer [39]. PANI due to its porous nature is considered a potential candidate for many applications [40].

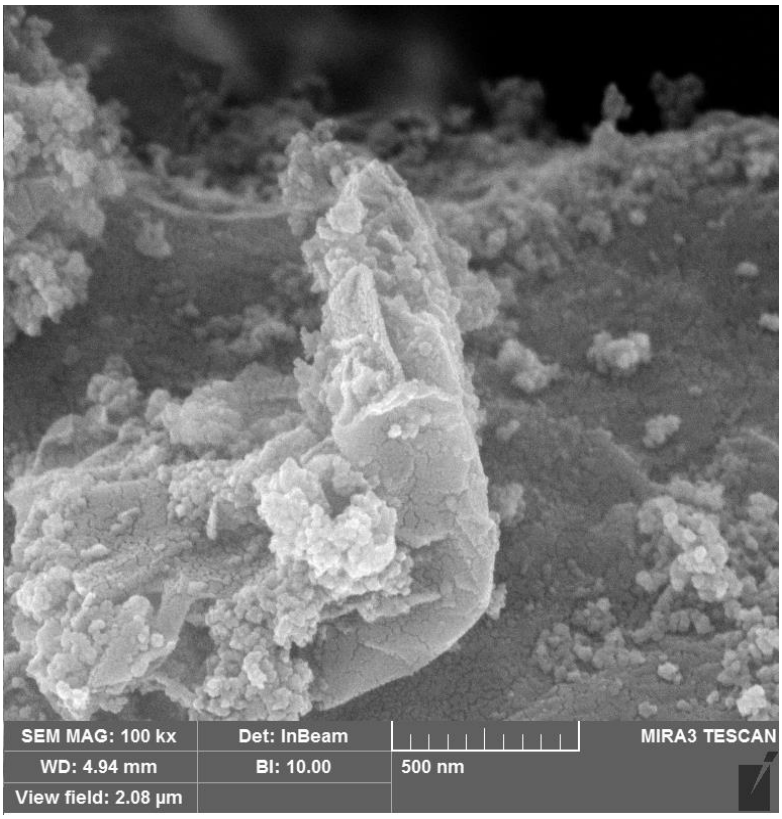

3.1.2 EDX spectroscopy

The percentage compositions of each constituent were assessed through the elemental composition analysis. It is observed that addition of low concentrations of Co_3O_4nanocubes in the polymeric matrix of PANI produced vague results with FESEM imaging. Therefore Energy dispersive X-ray spectroscopy was used as a reliable tool to assess the presence of cobalt oxide uniformly distributed throughout the nanocomposite material along with Oxygen, Nitrogen, Carbon and Iron. Fig. 2 displayed the elemental composition of the characterized material with a portion of 2.1% cobalt nanocube doped in polyaniline.

Elements	Weight%
C	26.32
N	45.45
O	21.44
Fe	3.69
Co	2.10
Total	100.00

3.1.3 FTIR spectroscopy

The presence of the following characteristic bands A, B and C cm^{-1} corresponding to PANI, magnetite and cobalt respectively confirmed the formation of the desired nanocomposite. FT-IR implies that the interaction between the dopants and PANI is based on the formation of bond ().

Fig. 3 represented the FT-IR spectra of Cobalt oxide nanocubes, PANI and PANI-Co4 nanocomposite. The spectra obtained for above mentioned materials exhibited band at 3431cm^{-1} which corresponds to the N-H stretching vibration in PANI polymer. The bands obtained at 1515 and 1420 cm^{-}represented the presence of C-C stretchings of quinoid and benzenoid rings in PANI that indicated the conductive emeraldine from PANI. The IR band at1297 and1560 cm^{-1}represnted the characteristic C-N and C=N stretching in PANI. The spinel structure of Co_3O_4 was confirmed by the presence of two bands at 667 and 574 cm^{-1} and band at 581 cm^{-1}represnted iron oxide (Fe-O) stretching vibration which confirmed the successful magnetization and the presence of magnetic nanoparticles in the nanocomposite product [33] + my paper as citation

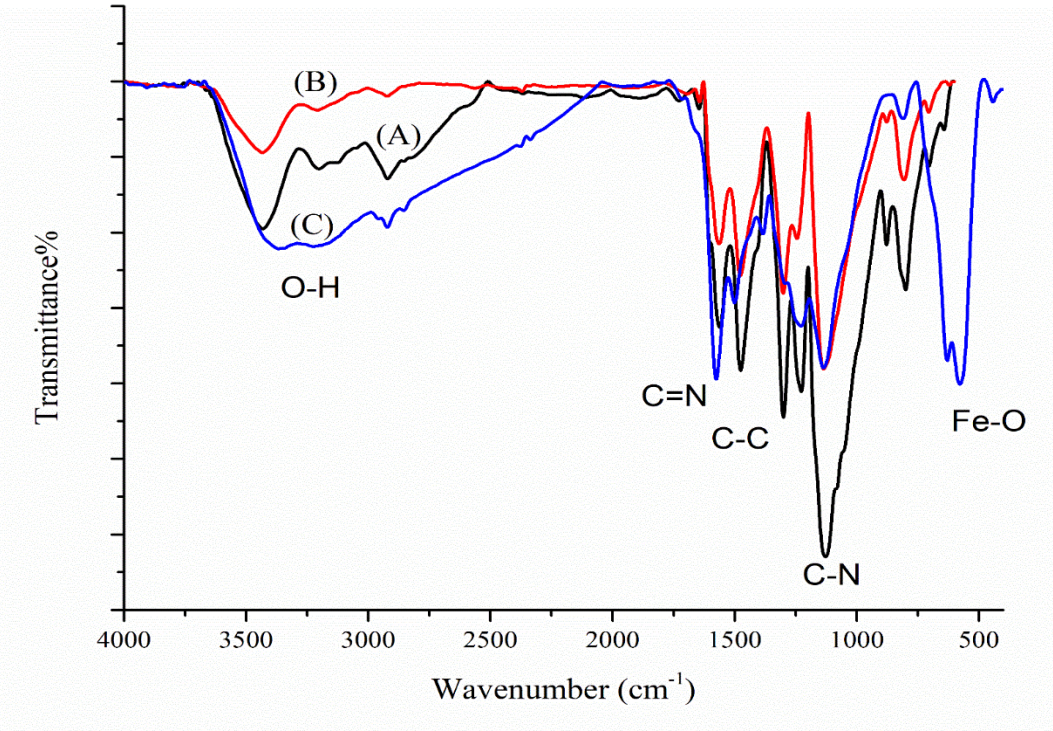

3.2 Parametric study

3.2.1 Effect of pH

The degree of nitrate adsorption depends on the pH due to the presence of various functional groups that adhere over the surface of the sorbent that acts as a function for the pH sample and contribute towards the surface charge of the nanocomposite as a whole and the interaction between the sorbent and the molecules to be analyzed in return [41].

Nitrate degradation studies showed that active sites present on the surface were activated more in acidic solutions [42] rendering a rapid kinetics [43]. To investigate the effect of initial pH on nitrate removal, diluted HCl (0.1 M) and NaOH (0.1 M) were taken to set the initial pH of the nitrate aqueous solution within the range of 2-10. According to the results obtained in Fig. 4, it was observed that the removal % of nitrate remained constant throughout the acidic and neutral solutions; however, after pH 6, a decrease from 90 to 60% was observed which implied that the maximum removal % can be achieved by keeping the pH within acidic or neutral range. The remarkably high initial adsorption capability of the reported nanocomposite were due to the presence of the positive surfaces of all three components namely polyaniline, cobalt and magnetite (oxides in general) at acidic pH which sustained the attractive electrostatic interaction between the positive sorbent and the negative nitrate ions [41], [44]. While, the low adsorption efficiency at high pH values, had occurred due to the increasing competition between the coexisting OH^- and nitrate ions for the active sites of the sorbent [29], [45]. It is important to note that PANI developed a positive charge in acidic environment due to the presence of basic amine and imine groups. Therefore at acidic pH the occurrence of the protonated

MO nanoparticles and the positively charged PANI-CoO4 nanocomposites lead to an increased adsorption efficiency through the sustained electrostatic attraction between the positive sorbent and the negative analyst ions which predominantly existed in anionic or neutral form (when NO- ions are protonated) due to the pKa of NO- higher than pH[46].

3.2.2 Effect of adsorbent dosage

Another important parameter is the dosage of adsorbent. Generally increase in the mass of adsorbent increases the active sites available for nitrate accommodation and removal. In the present study, the adsorbent mass varied within the range of 5 to 150 mg to figure out the highest possible efficiency with the most appropriate adsorbent amount. As shown in Fig. 5, the adsorption efficiency increased from 55 to 90 % to attain a steady state with constant trend thereafter at 60 mg. The increase can be explained in terms of the increase availability of adsorption sites with the increased in mass of the solid phase, while the constant level is observed probably due to the attainment of the saturation state of sorbent with the overlapping with the active sites and accumulation of nanoparticles at high sorbent dosages causing a decrease in the surface area and thus keeping the adsorption efficiency unchanged [47].

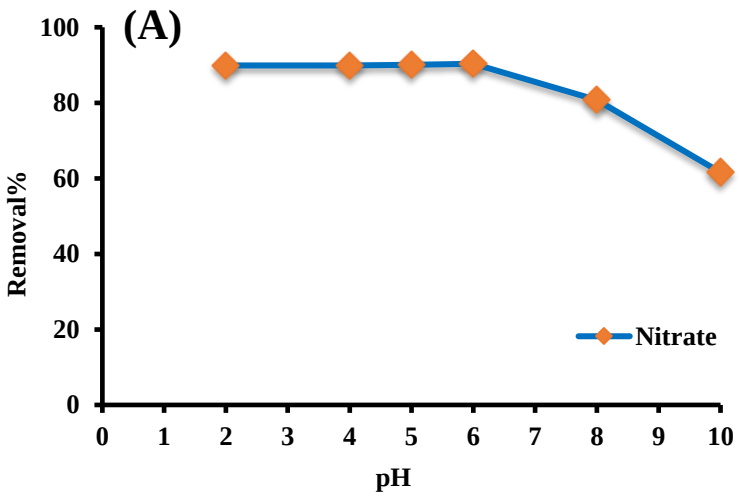

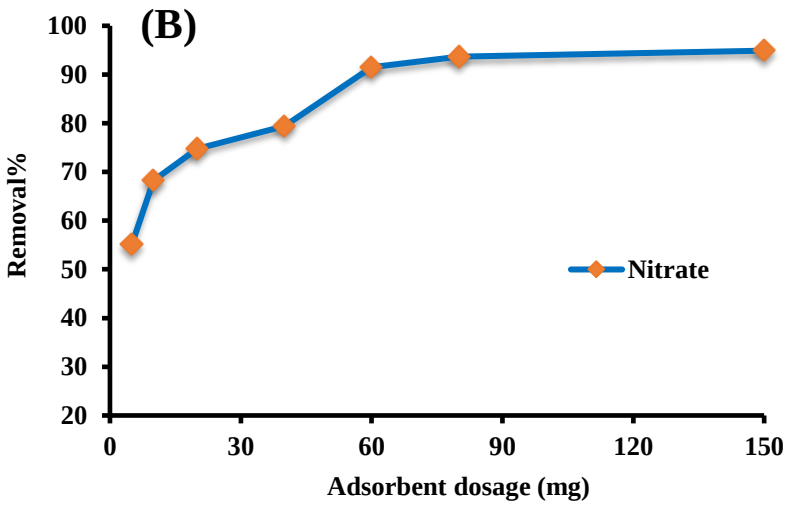

3.3 Time and adsorption kinetic

Kinetics underlying the removal process was investigated by varying the adsorption time from 5 to 150 minutes as represented in Fig. 4a. It was observed that adsorption of nitrate attained equilibrium (10 % removal efficiency) soon after 60 min and further increase in the contact time left PANI-Co_3O_4@MNPs adsorption capacity unchanged. The adsorption process proceed with increased rate initially due to presence of high availability of adsorbent sites at the beginning of the experiment that abruptly decreased to attain a plateau at contact time of 60 minutes due to substantial decrease in the number of available sites (saturation) and the analyst concentration. The rate of sorption and the mechanism for removal of nitrate to PANI-Co_3O_4@MNPs were described by the three kinetic models namely pseudo-first order, pseudo second-order and intra particle diffusion models. According to the pseudo first order, it is well known that the rate determining step for adsorption is linked with the physisorption process instead of electron sharing based-chemisorption process as stated by the pseudo second order kinetic model [27][28][29]. The intra particle diffusion model generally relates with the porous materials in which the transport and the adsorption of analyst is based on diffusion inside the sorbent (not at the surface) and within the pores (internal sites).The linear forms of the three kinetic models can be estimated according to the rate equations (3), (4) and (5), respectively.

$$\ln(Q_e - Q_t) = \ln Q_e - k_1 t \quad (3)$$

$$t/Q_t = 1/(k_2 Q_e^2) + t/Q_e \quad (4)$$

$$Q_t = k_{id}\sqrt{t} + I \quad (5)$$

where Q_e represented the equilibrium adsorption capacity(mg/g), Q_t signified the adsorption capacity at any time t, *I* denoted the intercept, k_1 (1/min), k_2(g/mg.min) and k_{id}(mg/g.√min) represented the first, second and intra-particle diffusion model rate constants, respectively. Plots between ln(Qe-Qt) versus t, t/Qt versus t and Q_t vs √t (Fig. 4B) represented the linear forms of data and provided the best fit for experimental measurements [27]

As per the results obtained and the simulation study of adsorption, the kinetic order followed the sequence (based on the higher R^2 value); pseudo first> pseudo second> intra particle with the experimental data exhibiting best fit with the kinetic model.

The kinetic parameters values such as coefficient of determination (R^2) and sorption capacities (Qe&Qt) are summarized in Table 1. The best model was selected by considering the highest R^2 value, the experimental capacity at equilibrium (Qe, exp) and the calculated one (Qe, cal). Hence, Table 1 revealed that the adsorption of Nitrate ions onto **PANI-Co_3O_4@MNPs** nanocomposites followed the pseudo-second-order kinetic model by displaying the highest R^2 value among all (0.964).

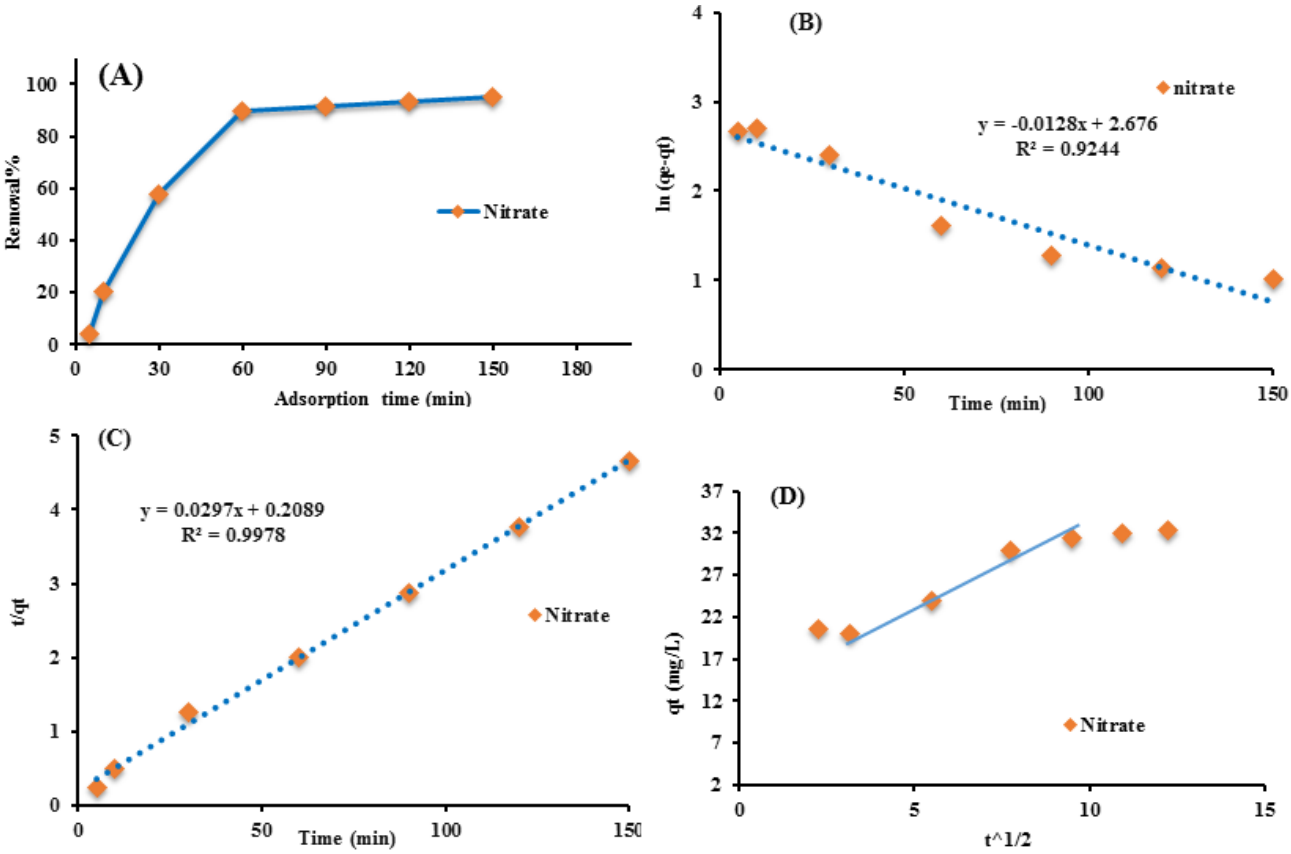

Fig. 4 (a) Effect of contact time, (b) pseudo first order (c) pseudo second order and (d) intra particle kinetic modeling of nitrate adsorption

3.4 Adsorption isotherm

Another crucial factor affecting the performance and the adsorption capacity (Qe) of the sorbent is the initial concentration of the analyst. For establishing the relation between Qe (mg/g) and the initial concentration of analyte Ce (mg/L), for the liquid in contact with the solid sorbent phase adsorption isotherms studies are necessary. The concentrations of nitrate ions varied from 10 to 250 mg/L and its effect on the removal process was studied. As shown in Fig. 5(A), it was observed that the curve exhibited increasing trend with a sharp slope initially followed by a slightly less sharp increase in which Qe raised from 4.98 to 65.15 mg/g as Ce increased from 1 to 25 mg/L. Thereafter, the increasing concentration had no effect on the adsorption capacity due to the attainment of the saturation state of the sorbent. Such observations revealed that nitrate removal onto **PANI-Co_3O_4@MNPs** is a type I adsorption process (according to IUPAC regulation) exhibiting only a single layer pattern of adsorbate over the sorbent surface[48].

In order to study the adsorption isotherm of the nitrate removal, two well-known models namely, Langmuir and Freundlich isotherms were adopted to figure out the most possible adsorption pattern and the maximum uptake capacity (Qm) of **PANI-Co_3O_4@MNPs** for nitrate at different Ce. Langmuir suggested that the sorbent behaved ideally having homogeneous surface and equivalent sites, therefore during the adsorption process (i) adsorbate displayed no phase transitions, (ii) energy of adsorption remained conserved and (iii) only single layer of solute is formed on the sorbent surface. On the other hand, Freundlich isotherm displayed the multilayered (physisorption) pattern for the adsorption mechanism.

The two models can be expressed linearly according to following equations (5) and (6), respectively.

$$C_e/Q_e = C_e/Q_m + 1/k_L Q_m \quad (5)$$

$$\ln Q_e = \ln K_F + (1/n) \ln C_e \quad (6)$$

where Qm (mg/g) represented the maximum monolayer adsorption capacity of sorbent, Qe (mg/g) represented the adsorption capacity at equilibrium, k_L(L/mg) and k_F[(mg/g)(L/mg)$^{1/n}$] represented the Langmuir and Freundlich model constants respectively (these constants measures the affinity of the sorbent towards the analyte and the adsorption capacity), Ce (mg/L) represented the residual concentration of nitrate after adsorption and 1⁄n is an another constant which measures the intensity and rate of occurrence of the adsorption process (Sayğılı and Güzel 2016). Fig. 5 (A-C) displayed linear plots for the both isotherms modelsLangmuir (B) and Freundlich (C) which showed that the experimental data linearly fitted linearly with respect to both models but exhibited relatively higher

R^2 value for Freundlich model which revealed that the nitrate adsorption and removal onto **PANI-Co_3O_4@MNPs** had followed the multilayer adsorption pattern.

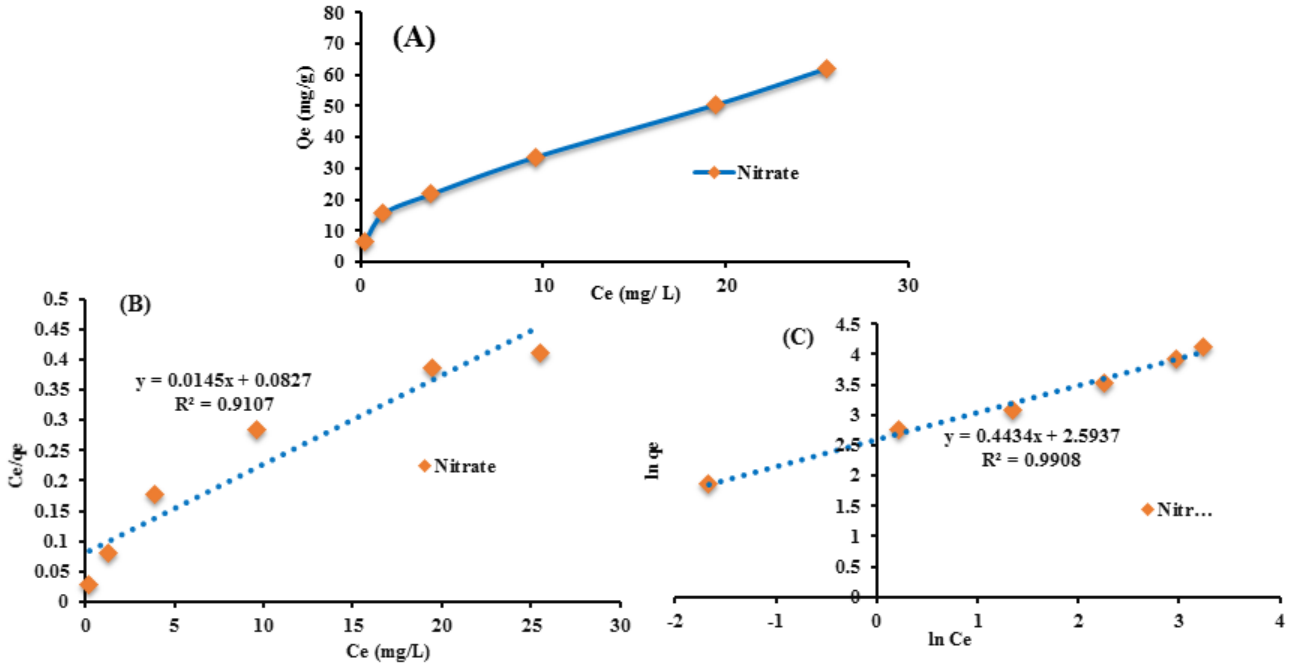

3.5 Thermodynamic and temperature

In this following section, various thermodynamic parameters involved in the nitrate adsorption process such as changes in enthalpy (ΔH^o, KJ/mol), entropy (ΔS^o,KJ/mol.^{o}K) and gibbs free energy (ΔG^o, KJ/mol) have been evaluated and represented in Table 4. Calculations were made on basis of graphs plotted between Gibbs free energy and the Equilibrium adsorption capacity for the material measured at different temperatures 20^{o}C, 25^{o}C and 35^{o}C. The expressions for the desired parameters can be evaluated using following equations:-

$$\Delta G^o = -RT ln\, K^o \qquad (7)$$

$$\Delta G^o = \Delta H^0 - T\Delta S^o \qquad (8)$$

where T represented the absolute temperature (^{o}C), R corresponded to the molar ideal gas constant (8.314 J. $mol^{-1}.K^{-1}$), and K^o signified the Langmuir constant (L/mol) which can be measured through the intercept of the plot drawn between C_e / q_e vs. C_e. It was evident from the decreased in in ΔG^0value with the increase in temperature and its negative value that the nitrate adsorption process has been spontaneous in nature and highly feasible via simple physical forces (Table. 4). The values of other parameters such as ΔH^o and ΔS^o can be estimated using the following Van't Hoff equation

$$lnK^o = \frac{\Delta S^o}{R} - \frac{\Delta H^o}{RT}$$

By plotting the Van't Hoff equation (lnK^o vs 1/T) the enthalpy (slope= ΔH^o/R) and entropy (intercept= ΔS^o/R) changes were estimated [49]. As shown in Table 4, negative values for both ΔH^0andΔS^0 revealed that the adsorption of nitrate is an exothermic process. Thus, increase in the temperature

favored the process in the backward direction leading to the decrease in the efficiency and adsorption capacity of the sorbent, whereas the negative value of the entropy signified decrease in the randomness of the solid-liquid solution interface system during the interaction of the analyst with the sorbent surface. The rate of the adsorption process thus decreased resulting in the lowering of contact and sorbent capacity and decrease in number of the nitrate ions need to be removed.

Table 4 The thermodynamic parameters of the adsorption of Nitrate onto **PANI-Co_3O_4@MNPs**

Temp °C	**Qe (mg/g)**	**ΔG**	**ΔH**	**ΔS**
20	32.5902	-9.26518	-49.6504	-0.1353
25	32.13067	-8.23054		
35	31.2749	-7.13059		

3.6 Regeneration

Regeneration is one of the prominent processes which describe the applicability and the suitability of the sorbent to be used economically over large scale for removal applications. In this study, the regeneration capability of **PANI-Co_3O_4@MNPs** was investigated by carrying out various adsorptions-desorption transitions and measuring the residual amount of the nitrate ions after each cycle. As shown in Fig. 8, the synthesized sorbent displayed a very high regeneration capacity of approximately 8 times before losing its efficiency in removal of nitrates.

3.7 Mechanism

The adsorption mechanism of nitrate for the given material can be evaluated both chemically and physically primarily on basis of the formation of a single layer of adsorbate at the surface sustained by chemisorption in accordance with the pseudo second order kinetic model, followed by the addition of more layers via the electrostatic interaction existing between the negatively charged nitrate ions and the positively charged sorbent material and thus, leading to the formation of the multilayer adsorption pattern as demonstrated by the Freundlich adsorption isotherm model.

Fig???

3.8 Comparison

The **PANI-Co_3O_4@MNPs** sorbent synthesized in the present study has been compared with the previously reported materials used in removal of nitrates in terms of performance and efficiency**.** As shown in Table 56], the performance of the synthesized material was found to be more effective in comparison with the other reported sorbents for the removal of nitrate in terms of adsorption capacity, sorbent dosage, simplicity, cost effectiveness, rapidness and adsorption capacity (Qe). The newly synthesized **PANI-Co_3O_4@MNPs** provides relatively high adsorption capacity (67.11 mg/g) at pH 6 compared with those of polyaniline@Fe3O4 (pH 8), polyaniline/polystyrene (pH 6), Fe-Mn/chitosan (pH 7), and Fe3O4/Zr(OH)2/chitosan (pH 6) with the privilege for easy isolation, fast adsorption kinetic, cheapness and low mass dosages. The much higher adsorption capacity of the zero valent iron based nanocomposite (polyaniline@Fe0 and Fe0/PVA/chitosan) is probably due to Fe–O–As interactions or synergistic effect of iron and polyaniline/chitosan. Nevertheless, the MPSrTiO3 nanocomposite provides an appropriate adsorption capacity for arsenic (III) removal from water samples comparing to polyaniline@Fe0 and Fe0/PVA/chitosan.

Table 5 Comparison study

Adsorbent	**PH**	**Time (min)**	**Qe (mg/g)**	**Ref.**
Chitosan PEG composite	**3**	**60**	**50.68**	[42]
Chitosan PVA composite	**3**	**60**	**30**	[42]
Magnetic graphene (nanosized lanthanum hydrous)	**6-8**	**30**	**138.88**	[43]
				Thisstudy

4 Conclusions

A very simple and economically oriented sorbent **PANI-Co_3O_4@MNPs** magnetic nanocomposite has been synthesized for the rapid and effective removal of harmful nitrates from underground water. **PANI-Co_3O_4@MNPs** has been investigated for its possible removal application and the most suitable parameters were studied to obtain the highest performance of the material for removal of nitrate from aqueous samples. The adsorption process was evaluated for kinetic, adsorption isotherms and thermodynamic and the results so obtained revealed that Freundlich isotherm and pseudo-first-order mostly fitted for the nitrate having relatively high adsorption capacity (67.11 mg/g) at pH 6 and spontaneous adsorption nature. The models suggested a multilayer adsorption pattern based on an exothermic physisorption adsorption process over the surface of **PANI-Co_3O_4@MNPs**. The high

removal efficiency (95.24% at pH 6) and regeneration potential of the material indicated that the proposed method can economically and potentially be use for large-scale environmental applications.

Acknowledgment

References

[1] P. Mikuška and Z. Večeřa, "Simultaneous determination of nitrite and nitrate in water by chemiluminescent flow-injection analysis," *Anal. Chim. Acta*, vol. 495, no. 1–2, pp. 225–232, Oct. 2003.

[2] M. A. Salam, O. Fageeh, S. A. Al-Thabaiti, and A. Y. Obaid, "Removal of nitrate ions from aqueous solution using zero-valent iron nanoparticles supported on high surface area nanographenes," *J. Mol. Liq.*, vol. 212, pp. 708–715, Dec. 2015.

[3] M. Keshvardoostchokami, S. Babaei, F. Piri, and A. Zamani, "Nitrate removal from aqueous solutions by ZnO nanoparticles and chitosan-polystyrene–Zn nanocomposite: Kinetic, isotherm, batch and fixed-bed studies," *Int. J. Biol. Macromol.*, vol. 101, pp. 922–930, Aug. 2017.

[4] Z. Jin, Z. Pan, M. Jin, F. Li, Y. Wan, and B. Gu, "Determination of nitrate contamination sources using isotopic and chemical indicators in an agricultural region in China," *Agric. Ecosyst. Environ.*, vol. 155, pp. 78–86, Jul. 2012.

[5] R. Grommen, I. Van Hauteghem, M. Van Wambeke, and W. Verstraete, "An improved nitrifying enrichment to remove ammonium and nitrite from freshwater aquaria systems," *Aquaculture*, vol. 211, no. 1–4, pp. 115–124, Aug. 2002.

[6] W. R. Melchert, C. M. C. Infante, and F. R. P. Rocha, "Development and critical comparison of greener flow procedures for nitrite determination in natural waters," *Microchem. J.*, vol. 85, no. 2, pp. 209–213, Apr. 2007.

[7] A. Afkhami, "Adsorption and electrosorption of nitrate and nitrite on high-area carbon cloth: an approach to purification of water and waste-water samples," *Carbon N. Y.*, vol. 41, no. 6, pp. 1320–1322, Jan. 2003.

[8] S. Tyagi, D. Rawtani, N. Khatri, and M. Tharmavaram, "Strategies for Nitrate removal from aqueous environment using Nanotechnology: A Review," *J. Water Process Eng.*, vol. 21, pp. 84–95, 2018.

[9] C. J. Mena-Duran, M. R. Sun Kou, T. Lopez, J. A. Azamar-Barrios, D. H. Aguilar, M. I. Domínguez, J. A. Odriozola, and P. Quintana, "Nitrate removal using natural clays modified by acid thermoactivation," *Appl. Surf. Sci.*, vol. 253, no. 13, pp. 5762–5766, Apr. 2007.

[10] A. Bhatnagar and M. Sillanpää, “A review of emerging adsorbents for nitrate removal from water,” *Chem. Eng. J.*, vol. 168, no. 2, pp. 493–504, Apr. 2011.

[11] P. Loganathan, S. Vigneswaran, and J. Kandasamy, “Enhanced removal of nitrate from water using surface modification of adsorbents – A review,” *J. Environ. Manage.*, vol. 131, pp. 363–374, 2013.

[12] C. M. Mendez, H. Olivero, D. E. Damiani, and M. A. Volpe, “On the role of Pd β-hydride in the reduction of nitrate over Pd based catalyst,” *Appl. Catal. B Environ.*, vol. 84, no. 1–2, pp. 156–161, Oct. 2008.

[13] S. Samatya, N. Kabay, Ü. Yüksel, M. Arda, and M. Yüksel, “Removal of nitrate from aqueous solution by nitrate selective ion exchange resins,” *React. Funct. Polym.*, vol. 66, no. 11, pp. 1206–1214, Nov. 2006.

[14] F. S. Fateminia and C. Falamaki, “Zero valent nano-sized iron/clinoptilolite modified with zero valent copper for reductive nitrate removal,” *Process Saf. Environ. Prot.*, vol. 91, no. 4, pp. 304–310, Jul. 2013.

[15] L. Durivault, O. Brylev, D. Reyter, M. Sarrazin, D. Bélanger, and L. Roué, “Cu–Ni materials prepared by mechanical milling: Their properties and electrocatalytic activity towards nitrate reduction in alkaline medium,” *J. Alloys Compd.*, vol. 432, no. 1–2, pp. 323–332, Apr. 2007.

[16] R. Epsztein, O. Nir, O. Lahav, and M. Green, “Selective nitrate removal from groundwater using a hybrid nanofiltration–reverse osmosis filtration scheme,” *Chem. Eng. J.*, vol. 279, pp. 372–378, Nov. 2015.

[17] Z. Zhang, Y. Xu, W. Shi, W. Wang, R. Zhang, X. Bao, B. Zhang, L. Li, and F. Cui, “Electrochemical-catalytic reduction of nitrate over Pd–Cu/γAl2O3 catalyst in cathode chamber: Enhanced removal efficiency and N2 selectivity,” *Chem. Eng. J.*, vol. 290, pp. 201–208, Apr. 2016.

[18] J. Martínez, A. Ortiz, and I. Ortiz, “State-of-the-art and perspectives of the catalytic and electrocatalytic reduction of aqueous nitrates,” *Appl. Catal. B Environ.*, vol. 207, pp. 42–59, 2017.

[19] Z. Shen, Y. Zhou, and J. Wang, “Comparison of denitrification performance and microbial diversity using starch/polylactic acid blends and ethanol as electron donor for nitrate removal,” *Bioresour. Technol.*, vol. 131, pp. 33–39, Mar. 2013.

[20] T. Kodera, S. Akizuki, and T. Toda, “Formation of simultaneous denitrification and methanogenesis granules in biological wastewater treatment,” *Process Biochem.*, vol. 58, pp. 252–257, Jul. 2017.

[21] Y. Li, Y. Wang, L. Fu, Y. Gao, H. Zhao, and W. Zhou, “Aerobic-heterotrophic nitrogen removal through nitrate reduction and ammonium assimilation by marine bacterium Vibrio

sp. Y1-5," *Bioresour. Technol.*, vol. 230, pp. 103–111, Apr. 2017.

[22] D. O'Carroll, B. Sleep, M. Krol, H. Boparai, and C. Kocur, "Nanoscale zero valent iron and bimetallic particles for contaminated site remediation," *Adv. Water Resour.*, vol. 51, pp. 104–122, Jan. 2013.

[23] P. Li, K. Lin, Z. Fang, and K. Wang, "Enhanced nitrate removal by novel bimetallic Fe/Ni nanoparticles supported on biochar," *J. Clean. Prod.*, vol. 151, pp. 21–33, May 2017.

[24] N. Barrabés and J. Sá, "Catalytic nitrate removal from water, past, present and future perspectives," *Appl. Catal. B Environ.*, vol. 104, no. 1–2, pp. 1–5, Apr. 2011.

[25] P. Ganesan, R. Kamaraj, and S. Vasudevan, "Application of isotherm, kinetic and thermodynamic models for the adsorption of nitrate ions on graphene from aqueous solution," *J. Taiwan Inst. Chem. Eng.*, vol. 44, no. 5, pp. 808–814, 2013.

[26] S. Chatterjee, D. S. Lee, M. W. Lee, and S. H. Woo, "Nitrate removal from aqueous solutions by cross-linked chitosan beads conditioned with sodium bisulfate," *J. Hazard. Mater.*, vol. 166, no. 1, pp. 508–513, Jul. 2009.

[27] A. Sowmya and S. Meenakshi, "A novel quaternized chitosan–melamine–glutaraldehyde resin for the removal of nitrate and phosphate anions," *Int. J. Biol. Macromol.*, vol. 64, pp. 224–232, Mar. 2014.

[28] H. Jiang, P. Chen, S. Luo, X. Tu, Q. Cao, and M. Shu, "Synthesis of novel nanocomposite Fe3O4/ZrO2/chitosan and its application for removal of nitrate and phosphate," *Appl. Surf. Sci.*, vol. 284, pp. 942–949, 2013.

[29] W. Song, B. Gao, X. Xu, F. Wang, N. Xue, S. Sun, W. Song, and R. Jia, "Adsorption of nitrate from aqueous solution by magnetic amine-crosslinked biopolymer based corn stalk and its chemical regeneration property," *J. Hazard. Mater.*, vol. 304, pp. 280–290, 2016.

[30] X. Zhao, L. Lv, W. Zhang, S. Zhang, and Q. Zhang, "Polymer-supported nanocomposites for environmental application: A review," *Chem. Eng. J.*, vol. 170, no. 2–3, pp. 381–394, Jun. 2011.

[31] S. Bhadra, D. Khastgir, N. K. Singha, and J. H. Lee, "Progress in preparation, processing and applications of polyaniline," *Prog. Polym. Sci.*, vol. 34, no. 8, pp. 783–810, Aug. 2009.

[32] S. Shahabuddin, N. M. Sarih, F. H. Ismail, M. M. Shahid, and N. M. Huang, "Synthesis of chitosan grafted-polyaniline/Co3O4 nanocube nanocomposites and their photocatalytic activity toward methylene blue dye degradation," *RSC Adv.*, vol. 5, no. 102, pp. 83857–83867, 2015.

[33] H. Mohammadi Nodeh,Mohammad Kazem. Soltani, Sara. Shahabuddin, Syed. Rashidi Nodeh, Hamid. Sereshti, "Equilibrium, Kinetic and Thermodynamic Study of Magnetic Polyaniline/Graphene Oxide Based Nanocomposites for Ciprofloxacin Removal from

Water," *Inorg. Organomet. Polym. Mater.*, 2018.

[34] X. Lu, C. Y. Tan, J. Xu, and C. He, "Thermal degradation of electrical conductivity of polyacrylic acid doped polyaniline: effect of molecular weight of the dopants," *Synth. Met.*, vol. 138, no. 3, pp. 429–440, Jul. 2003.

[35] K. Takahashi, K. Nakamura, T. Yamaguchi, T. Komura, S. Ito, R. Aizawa, and K. Murata, "Characterization of water-soluble externally HCl-doped conducting polyaniline," *Synth. Met.*, vol. 128, no. 1, pp. 27–33, Apr. 2002.

[36] Shahabuddina, Syed. Muhamad Sarih, Norazilawati. Mohamada, Sharifah. Atika Baharin, "Synthesis and Characterization of Co3O4 Nanocube Doped Polyaniline Nanocomposites with Enhanced Methyl Orange Adsorption from Aqueous Solution," *RSC Adv.*, 2016.

[37] H. N. Shahid, Muhammad Mehmood. Pandikumar, Alagarsamy . Moradi Golsheikh, Amir . Huang, Nay Ming. Lim, "Enhanced electrocatalytic performance of cobalt oxide nanocubes incorporating reduced graphene oxide as a modified platinum electrode for methanol oxidation," *RSC Adv.*, vol. 4, pp. 62793–62801, 2014.

[38] S. Shahabuddin, N. M. Sarih, M. A. Kamboh, H. R. Nodeh, and S. Mohamad, "Synthesis of polyaniline-coated graphene oxide@SrTiO<inf>3</inf>nanocube nanocomposites for enhanced removal of carcinogenic dyes from aqueous solution," *Polymers (Basel).*, vol. 8, no. 9, 2016.

[39] A. A. Pud, O. A. Nikolayeva, L. O. Vretik, Y. V Noskov, N. A. Ogurtsov, O. S. Kruglyak, and E. A. Fedorenko, "New nanocomposites of polystyrene with polyaniline doped with lauryl sulfuric acid," *Nanoscale Res. Lett.*, vol. 12, no. 1, p. 493, 2017.

[40] D. K. Bandgar, G. D. Khuspe, R. C. Pawar, C. S. Lee, and V. B. Patil, "Facile and novel route for preparation of nanostructured polyaniline (PANi) thin films," *Appl. Nanosci.*, vol. 4, no. 1, pp. 27–36, 2014.

[41] F. Keyhanian, S. Shariati, M. Faraji, and M. Hesabi, "Magnetite nanoparticles with surface modification for removal of methyl violet from aqueous solutions," *Arab. J. Chem.*, vol. 9, pp. S348–S354, 2016.

[42] A. Rajeswari, A. Amalraj, and A. Pius, "Adsorption studies for the removal of nitrate using chitosan/PEG and chitosan/PVA polymer composites," *J. Water Process Eng.*, vol. 9, pp. 123–134, Feb. 2016.

[43] H. R. Nodeh, H. Sereshti, E. Z. Afsharian, and N. Nouri, "Enhanced removal of phosphate and nitrate ions from aqueous media using nanosized lanthanum hydrous doped on magnetic graphene nanocomposite," *J. Environ. Manage.*, vol. 197, pp. 265–274, 2017.

[44] N. Razavi and A. Sarafraz Yazdi, "New application of chitosan- grafted polyaniline in dispersive solid- phase extraction for the separation and determination of phthalate esters in

milk using high- performance liquid chromatography," *J. Sep. Sci.*, vol. 40, no. 8, pp. 1739–1746, 2017.

[45] S. Kilpimaa, H. Runtti, T. Kangas, U. Lassi, and T. Kuokkanen, "Physical activation of carbon residue from biomass gasification: Novel sorbent for the removal of phosphates and nitrates from aqueous solution," *J. Ind. Eng. Chem.*, vol. 21, pp. 1354–1364, 2015.

[46] S. Shahabuddin, N. M. Sarih, M. Afzal Kamboh, H. Rashidi Nodeh, and S. Mohamad, "Synthesis of polyaniline coated graphene oxide@SrTiO3 nanocube nanocomposites for enhanced Removal of carcinogenic dyes from aqueous solution," *Polymers (Basel).*, vol. 8, pp. 305–310, 2016.

[47] H. Rashidi Nodeh, H. Sereshti, E. Zamiri Afsharian, and N. Nouri, "Enhanced removal of phosphate and nitrate ions from aqueous media using nanosized lanthanum hydrous doped on magnetic graphene nanocomposite," *J. Environ. Manage.*, vol. 197, 2017.

[48] S. Shrestha, G. Son, S. H. Lee, and T. G. Lee, "Isotherm and thermodynamic studies of Zn (II) adsorption on lignite and coconut shell-based activated carbon fiber," *Chemosphere*, vol. 92, no. 8, pp. 1053–1061, 2013.

[49] F. Nekouei, S. Nekouei, I. Tyagi, and V. K. Gupta, "Kinetic, thermodynamic and isotherm studies for acid blue 129 removal from liquids using copper oxide nanoparticle-modified activated carbon as a novel adsorbent," *J. Mol. Liq.*, vol. 201, pp. 124–133, 2015.